TU Delft

Delft University of Technology

Comparison of Modular Multilevel Converter Based Solid State Transformer for AC/DC Application

Li, Zhengzhao; Qin, Zian; Mirzadarani, Reza; Niasar, Mohamad Ghaffarian; Itraj, Mahesh; Van Lieshout, Lou; Bauer, Pavol

DOI
10.1109/IECON51785.2023.10312314

Publication date
2023

Document Version
Final published version

Published in
IECON 2023 - 49th Annual Conference of the IEEE Industrial Electronics Society

Citation (APA)
Li, Z., Qin, Z., Mirzadarani, R., Niasar, M. G., Itraj, M., Van Lieshout, L., & Bauer, P. (2023). Comparison of Modular Multilevel Converter Based Solid State Transformer for AC/DC Application. In *IECON 2023 - 49th Annual Conference of the IEEE Industrial Electronics Society* (IECON Proceedings (Industrial Electronics Conference)). IEEE. https://doi.org/10.1109/IECON51785.2023.10312314

Important note
To cite this publication, please use the final published version (if applicable).
Please check the document version above.

Copyright
Other than for strictly personal use, it is not permitted to download, forward or distribute the text or part of it, without the consent of the author(s) and/or copyright holder(s), unless the work is under an open content license such as Creative Commons.

Takedown policy
Please contact us and provide details if you believe this document breaches copyrights.
We will remove access to the work immediately and investigate your claim.

This work is downloaded from Delft University of Technology.
For technical reasons the number of authors shown on this cover page is limited to a maximum of 10.

Green Open Access added to TU Delft Institutional Repository

'You share, we take care!' - Taverne project

https://www.openaccess.nl/en/you-share-we-take-care

Otherwise as indicated in the copyright section: the publisher is the copyright holder of this work and the author uses the Dutch legislation to make this work public.

Comparison of Modular Multilevel Converter based Solid State Transformer for AC/DC application

Zhengzhao Li
DC Energy Conversion and Storage
TU Delft
Delft, The Netherlands
Z.Li-20@tudelft.nl

Zian Qin
DC Energy Conversion and Storage
TU Delft
Delft, The Netherlands
Z.Qin-2@tudelft.nl

Reza Mirzadarani
High Voltage Technologies
TU Delft
Delft, The Netherlands
R.Mirzadarani@tudelft.nl

Mohamad Ghaffarian Niasar
High Voltage Technologies
TU Delft
Delft, The Netherlands
M.GhaffarianNiasar@tudelft.nl

Mahesh Itraj
VONK
Zwolle, The Netherlands
mahesh.itraj@iivonk.com

Lou Van Lieshout
VONK
Zwolle, The Netherlands
lou.vanlieshout@iivonk.com

Pavol Bauer
DC Energy Conversion and Storage
TU Delft
Delft, The Netherlands
P.Bauer@tudelft.nl

IECON 2023- 49th Annual Conference of the IEEE Industrial Electronics Society | 979-8-3503-3182-0/23/$31.00 ©2023 IEEE | DOI: 10.1109/IECON51785.2023.10312314

***Abstract*—For electrolyzer applications, traditional solutions using line frequency transformers plus rectifiers are bulky, heavy and have low controllability. The Solid State Transformer (SST) could be a promising solution to solve the mentioned issues. This paper compares the semiconductor ratings and capacitance of five different Modular Multilevel Converter (MMC) based Solid State Transformer (SST) topologies. The results show that the DRU (Diode Rectifier Unit)-MMC based topologies have the lowest semiconductor ratings and capacitance. Because of the unidirectional power flow requirement, the source side MMC of Back-to-Back (BtB) MMC based SST could be replaced by DRU, thus the cost is drastically saved. Another interesting finding is that the DRU-MMC energy ripple is much lower than half of the energy ripple in BtB MMC, which is different from HVDC MMC.**

Keywords—Modular Multilevel Converter, Solid State Transformer, Electrolyzer

I. INTRODUCTION

Hydrogen electrolyzer is getting more and more popularity because of its capability to provide flexibility to the energy system to facilitate the integration of intermittent energy sources, like solar and wind power. Besides, it could contribute the sustainability by delivering carbon-free hydrogen to other sectors, like industry and mobility sector.

The current power conversion method of hydrogen production is by using line frequency transformer to step down the AC voltage together with thyristor or Diode Rectifier Unit (DRU) rectifier to generate the required DC voltage [1]. This method has two shortcomings. First it is bulky and heavy because of the usage of line frequency transformer, which might be problematic for transportation. The second issue is that it lacks controllability, especially when facing intermittent renewable power generations. In this scenario, an optimal control of electrolyzer is required to maximize the hydrogen generation and to balance the power generated by renewable energy and the power required by electrolyzer.

This project has received funding from the RVO MOOI (Missiegedreven Onderzoek Ontwikkeling en Innovation) under grant agreement MOOI 52103.

To address these issues, the Solid State Transformer (SST) is a promising solution. The fundamental idea of SST is to use converters to convert the input fundamental frequency AC voltage into medium frequency (MF) or high frequency (HF) AC voltages, and then use MF/HF transformer to step down the voltages. Because the transformer size and weight are inversely proportional to its operating frequency, the SST is much lighter and smaller compared to the line frequency transformer plus rectifier. And the controllability of SST is also higher than the traditional solutions.

For the AC-DC SST, there are mainly two types of solutions. The most popular one is the cascaded topology [2]. Because of the high input voltage and high output current requirement of the electrolyzer system, usually the input series and output parallel (ISOP) structure is used. The main disadvantage of this topology is that each module has one MF transformer. And these transformers need to withstand the whole range of the input voltage. And the total size of the transformers is large because of thick insulations.

Another possible SST solution is using Modular Multilevel Converter (MMC) to interface the high input voltage. The MMC based SST structure requires only one MFT. Thus the size and weight of this single MFT should be smaller than the aforementioned small MFTs in cascaded structure combined.

Various papers have compared different MMC structures for AC/AC applications [3-7], from semiconductor rating and capacitance points of view. However, there is a lack of attention to the comparison of MMC based AC-DC converter topologies.

This paper focuses on the MMC semiconductor rating and capacitance comparison of AC-DC SST for electrolyzer applications. Section II presents MMC based AC-DC SST topology candidates. Section III and Section IV calculate the required semiconductor ratings and equivalent capacitance requirements for different topologies, respectively. Section V summarizes the calculation results, and by comparing ratings of different topologies, the most suitable one is chosen for future research.

Authorized licensed use limited to: TU Delft Library. Downloaded on April 03,2024 at 06:49:34 UTC from IEEE Xplore. Restrictions apply.

II. Topology Candidates

Several MMC based SST could be used for AC-DC applications, as shown in Fig. 1 - Fig. 5.

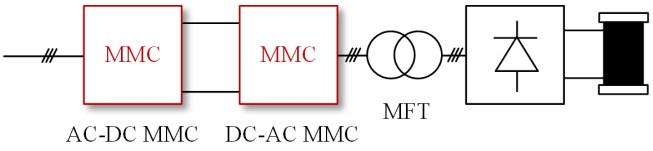

Fig. 1. Back to Back MMC based SST

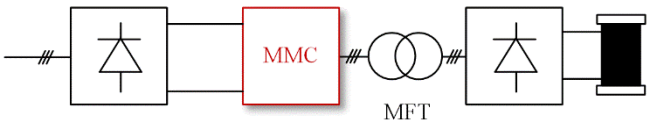

Fig. 2. DC-3ΦAC MMC based SST

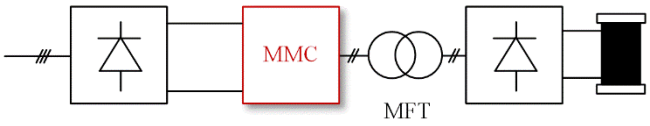

Fig. 3. DC-1ΦAC MMC based SST

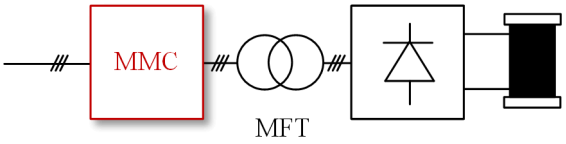

Fig. 4. 3ΦAC-3ΦAC MMC based SST

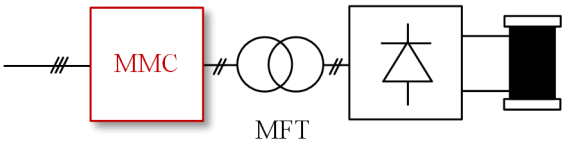

Fig. 5. 3ΦAC-1ΦAC MMC based SST

The most commonly used one is the back-to-back MMC. But for the unidirectional load applications such as hydrogen electrolyzer, the back-to-back configuration which is especially suitable for bidirectional power flow seems like a waste of its full capability.

Thus the front side AC-DC MMC could be replaced by DRU to save a vast number of power switches cost, as shown in Fig. 2.

And there also exists another level of freedom, which is the number of phases of medium frequency transformer (MFT). Thus by replacing the three phase MFT and DC-3Φ AC MMC with 1Φ MFT and DC-1ΦAC MMC, another possible solution is exhibited in Fig. 3.

Other possible solutions are direct AC-AC MMC [8], which are said to be promising solutions to replace the traditional back to back MMC, because of the simplicity of the structure and reduced number of energy conversion stages, as shown in Fig. 4. Similar to Fig. 3, if 1Φ MFT is used, a 3ΦAC-1ΦAC MMC based SST could be considered for comparison.

It should be noted that for the following semiconductor rating calculation and comparison, the semiconductor rating of the DRU connected to the secondary side of the MFT is not analyzed, because the same DRU block will always exist in every topology. And because the front-side DRUs in Fig. 2 and Fig. 3 are considerably cheaper compared to the MMC, thus the cost of them is omitted as well.

For the capacitor rating calculation, since there are no main DC link capacitors in each topology but separated capacitors in every MMC submodule, MMC capacitor rating of every topology is the total capacitor rating.

In short, the semiconductor and capacitor ratings calculations for solid state transformer in the following sections focus on the MMC block.

III. Semiconductor Rating Calculation

A. Overall calculation method

The semiconductor cost depends mainly on its rated switching power, by multiplying maximum current and maximum voltage. For every SST topology the total switching power of MMC could be calculated as follows [6]:

$$S_{total} = n_{arm} n_{sm} U_{arm\_\max} I_{arm\_\max}$$

Where n_{arm} represents number of arms, n_{sm} represents number of semiconductors per submodule, U_{arm_max} represents maximum arm voltage, and I_{arm_max} represents maximum arm current.

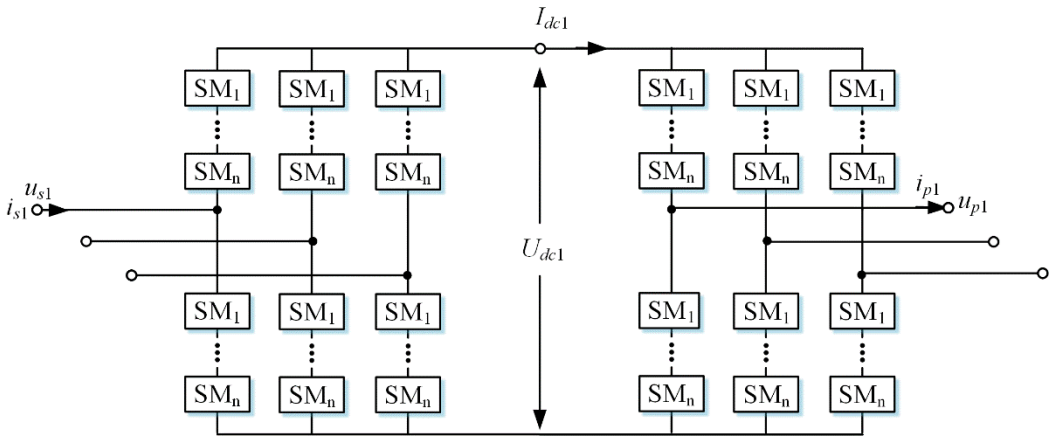

Fig. 6. Back to back MMC

Authorized licensed use limited to: TU Delft Library. Downloaded on April 03,2024 at 06:49:34 UTC from IEEE Xplore. Restrictions apply.

As shown in [3], when the modulation index equals 1, the semiconductor rating and capacitor rating is the lowest. Thus except for the direct AC-AC MMC, the modulation indexes in all other MMC in the SST topologies are considered as 1.

For MMC applications, harmonic injection method could be used to increase the modulation range of the MMC. However, for the simplicity of comparison procedure, the harmonic injection is omitted [7].

The system has a 33 kV line to line input voltage and the total power is 45 MW. An initial selection of the solid state transformer operating frequency is chosen as 400 Hz. It should be noted that the calculation procedure could also be applied to the system with different voltage/power configurations, by simply replacing the values.

B. Calculation process

For a better explanation, the MMC parts of Fig. 1 to Fig. 5 are drawn in Fig. 6 to Fig. 10. The input source voltage of MMC is $u_{s1} = 26.9\cos(2\pi \times 50t)$ kV and the input current is $i_{s1} = 1.11\cos(2\pi \times 50t)$ kA . Thus the DC link voltage and current shown in Fig. 6 could be calculated as

$$U_{dc1} = 2U_{s1\max} = 53.7 \text{ kV} \tag{1}$$

$$I_{dc1} = \frac{P}{U_{dc1}} = 0.835 \text{ kA} \tag{2}$$

And the output AC voltage and current are

$$u_{p1} = 26.9\cos(2\pi \times 400t) \text{ kV} \tag{3}$$

$$i_{p1} = 1.11\cos(2\pi \times 400t) \text{ kA} \tag{4}$$

For the MMC connected to the source side, the arm current and arm voltage expressions are

$$u_{arm1} = \frac{U_{dc1}}{2} - u_{s1} = 26.9 - 26.9\cos(2\pi \times 50t) \text{ kV} \tag{5}$$

$$i_{arm1} = \frac{I_{dc1}}{3} + \frac{i_{s1}}{2} = 0.28 + 0.56\cos(2\pi \times 50t) \text{ kA} \tag{6}$$

The arm current and voltage peak values are

$$u_{arm1\_\max} = \frac{U_{dc1}}{2} + u_{s1\_\max} = 53.9 \text{ kV} \tag{7}$$

$$i_{arm1\_\max} = \frac{I_{dc1}}{3} + \frac{i_{s1\_\max}}{2} = 0.84 \text{ kA} \tag{8}$$

The total semiconductor rating for the source side MMC is

$$\begin{aligned} S_{source1} &= n_{arm1} n_{sm1} U_{arm1\_\max} I_{arm1\_\max} \\ &= 6 \times 2 \times 53.9 \text{ kV} \times 0.84 \text{ kA} = 540 \text{ MVA} \end{aligned} \tag{9}$$

Similarly, the load side MMC semiconductor ratings could be calculated, and the two results combined is

$$S_{total1} = 1080 \text{ MVA} \tag{10}$$

In (9), $n_{sm1} = 2$, meaning that the half bridge submodule is considered. In HVDC application, full bridge submodule is usually used to control the DC short circuit current. However, since there is no long DC transmission line in this SST application scenario, the probability of DC short circuit fault is low. Thus the half bridge submodule is preferred, and in case the DC short circuit fault happens, the mechanical switch and thyristor bypass switch connected to each submodule could handle the DC fault [9]. The same consideration is applied to the DC-3ΦAC MMC based SST and DC-1ΦAC MMC based SST.

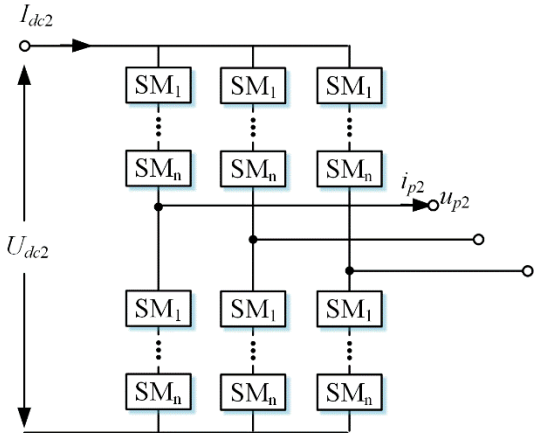

Fig. 7. DC-3ΦAC MMC

For DC-AC MMC based SST, since the voltage transfer ratio of DRU is π/3, thus $U_{dc2} = U_{dc3} = 44.6$ kV , and $I_{dc2} = I_{dc3} = 1.01$ kA . The arm voltage and arm current expressions for DC-3ΦAC MMC based SST are

$$u_{arm2} = \frac{U_{dc2}}{2} - u_{p2} = 22.3 - 22.3\cos(2\pi \times 400t) \text{ kV} \tag{11}$$

$$i_{arm2} = \frac{I_{dc2}}{3} + \frac{i_{p2}}{2} = 0.34 + 0.67\cos(2\pi \times 400t) \text{ kA} \tag{12}$$

The total semiconductor rating for this topology is

$$\begin{aligned} S_{total2} &= n_{arm2} n_{sm2} U_{arm2\_\max} I_{arm2\_\max} \\ &= 6 \times 2 \times 44.6 \text{ kV} \times 1.01 \text{ kA} = 540 \text{ MVA} \end{aligned} \tag{13}$$

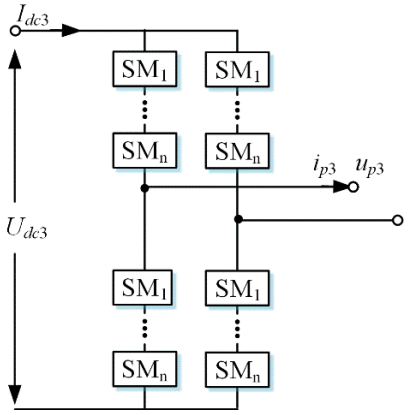

Fig. 8. DC-1ΦAC MMC

Authorized licensed use limited to: TU Delft Library. Downloaded on April 03,2024 at 06:49:34 UTC from IEEE Xplore. Restrictions apply.

The arm voltage, arm current, and total semiconductor rating expressions for DC-1ΦAC MMC are

$$u_{arm3} = \frac{U_{dc3}}{2} - \frac{u_{p3}}{2} = 22.3 - 22.3\cos(2\pi \times 400t) \text{ kV} \quad (14)$$

$$i_{arm3} = \frac{I_{dc3}}{2} + \frac{i_{p3}}{2} = 0.5 + \cos(2\pi \times 400t) \text{ kA} \quad (15)$$

$$\begin{aligned} S_{total3} &= n_{arm3} n_{sm3} U_{arm3\_\max} I_{arm3\_\max} \\ &= 4 \times 2 \times 44.6 \text{ kV} \times 1.5 \text{ kA} = 540 \text{ MVA} \end{aligned} \quad (16)$$

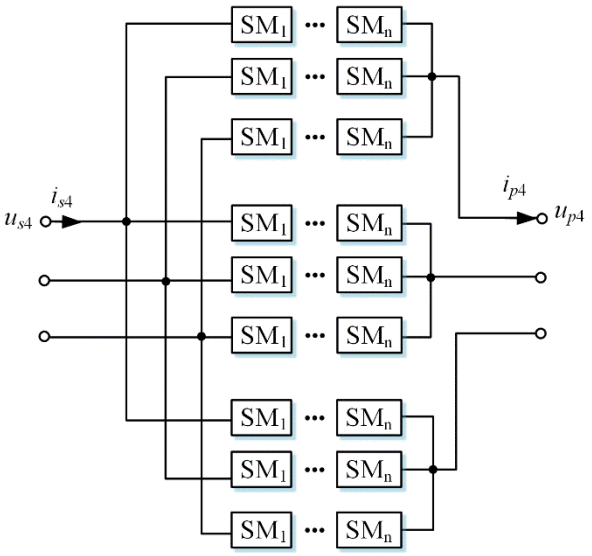

Fig. 9. 3ΦAC-3ΦAC MMC

For direct AC-AC MMC, full bridge submodule is required [10], which could increase the semiconductor ratings of the topology. Also two different frequency components flow through the arms, which increases the complexity of the control system [11].

Since the full bridge arm is used, the voltage transfer ratio p_1 between input and output could be arbitrary. The output phase voltage and phase current for 3ΦAC-3ΦAC MMC could be written as

$$u_{p4} = 26.9 p_1 \cos(2\pi \times 400t + \varphi) \text{ kV} \quad (17)$$

$$i_{p4} = \frac{1.11}{p_1} \cos(2\pi \times 400t + \varphi) \text{ kA} \quad (18)$$

The arm voltage and current expressions are

$$\begin{aligned} u_{arm4} &= u_{s4} - u_{p4} \\ &= 26.9\cos(2\pi \times 50t) - 26.9 p_1 \cos(2\pi \times 400t + \varphi) \text{ kV} \end{aligned} \quad (19)$$

$$\begin{aligned} i_{arm4} &= \frac{i_{s4}}{3} + \frac{i_{p4}}{3} \\ &= 0.37\cos(2\pi \times 50t) + \frac{0.37}{p_1} \cos(2\pi \times 400t + \varphi) \text{ kA} \end{aligned} \quad (20)$$

The total semiconductor rating is

$$\begin{aligned} S_{total4} &= n_{arm4} n_{sm4} U_{arm4\_\max} I_{arm4\_\max} \\ &= 9 \times 4 \times (26.9 + 26.9 p_1) \text{kV} \times \left(0.37 + \frac{0.37}{p_1}\right) \text{kA} \end{aligned} \quad (21)$$

The minimum total switching power is acquired when voltage transfer ratio p_1 equals 1

$$S_{total4\_\min} = 1440 \text{ MVA} \quad (22)$$

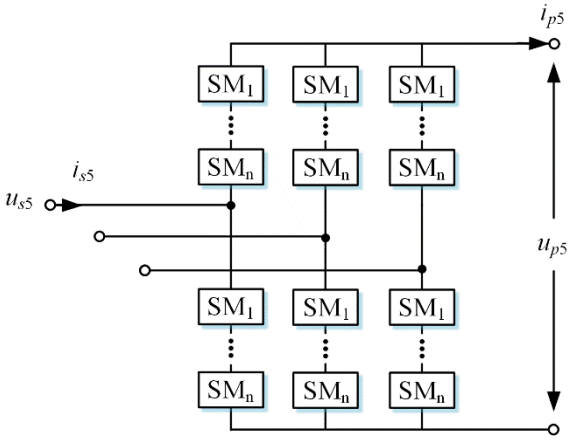

Fig. 10. 3ΦAC-1ΦAC MMC

Suppose the voltage transfer ratio of 3ΦAC-1ΦAC MMC is p_2

$$\begin{aligned} u_{arm5} &= u_{s5} - \frac{u_{p5}}{2} \\ &= 26.9\cos(2\pi \times 50t) - 13.5 p_2 \cos(2\pi \times 400t + \varphi) \text{ kV} \end{aligned} \quad (23)$$

$$\begin{aligned} i_{arm5} &= \frac{i_{s5}}{2} + \frac{i_{p5}}{3} \\ &= 0.56\cos(2\pi \times 50t) + \frac{1.11}{p_2} \cos(2\pi \times 400t + \varphi) \text{ kA} \end{aligned} \quad (24)$$

$$\begin{aligned} S_{total5} &= n_{arm5} n_{sm5} U_{arm5\_\max} I_{arm5\_\max} \\ &= 6 \times 4 \times (26.9 + 13.5 p_2) \text{kV} \times \left(0.56 + \frac{1.11}{p_2}\right) \text{kA} \end{aligned} \quad (25)$$

The minimum total switching power is acquired when voltage transfer ratio $p2$ equals 2

$$S_{total5\_\min} = 1440 \text{ MVA} \quad (26)$$

IV. Equivalent Capacitor Rating Calculation

A. Overall calculation method

The overall capacitance of each topology is directly related to the total energy variation [6]. By integrating the product of the arm voltage and arm current over time, the energy in one arm can be calculated

Authorized licensed use limited to: TU Delft Library. Downloaded on April 03,2024 at 06:49:34 UTC from IEEE Xplore. Restrictions apply.

$$e_{arm} = \int u_{arm} i_{arm} dt \tag{27}$$

The total energy for the whole MMC could be calculated as

$$e_{total} = n_{arm} \int u_{arm} i_{arm} dt \tag{28}$$

The total energy variation could be calculated as

$$\Delta e_{total} = \max\left(e_{total}(t)\right) - \min\left(e_{total}(t)\right) \tag{29}$$

In this paper, the total energy variation is used as a method to represent the required capacitance.

B. Calculation process

For back to back MMC shown in Fig. 6, the total energy of the source side MMC is

$$\begin{aligned} e_{total1\_source} &= n_{arm1} \int u_{arm1} i_{arm1} dt \\ &= 6 \int \left[26.9 - 26.9\cos(2\pi \times 50t)\right]\left[0.28 + 0.56\cos(2\pi \times 50t)\right] dt \\ &= 6 \times 26.9 \times 0.28 \int \left(\cos(100\pi t) - \cos(200\pi t)\right) dt \\ &= 6 \times 26.9 \times 0.28 \times \frac{1}{200\pi}\left[2\sin(100\pi t) - \sin(200\pi t)\right] \end{aligned} \tag{30}$$

Thus the total energy variation of the source side MMC is

$$\begin{aligned} \Delta e_{total1\_source} &= \max\left(e_{total1\_source}(t)\right) - \min\left(e_{total1\_source}(t)\right) \\ &= 372 \text{ kJ} \end{aligned} \tag{31}$$

Similarly the total energy variation of the load side MMC could be calculated, and the two results combined is

$$\Delta e_{total1} = 419 \text{ kJ} \tag{32}$$

During the derivation process, it is found that the energy variation of the source side MMC is constant because of the fixed 50 Hz input AC frequency, but the load side MMC energy variation is inversely proportional to the output AC frequency f_1. And the total energy variation related to f_1 could be written as

$$\Delta e_{total1} = 372 + \frac{18621}{f_1} \text{kJ} \tag{33}$$

For DC-3ΦAC MMC shown in Fig. 7, the total energy is

$$\begin{aligned} e_{total2} &= n_{arm2} \int u_{arm2} i_{arm2} dt \\ &= 6 \times 22.3 \times 0.34 \int \left(\cos(800\pi t) - \cos(1600\pi t)\right) dt \\ &= 6 \times 22.3 \times 0.34 \times \frac{1}{1600\pi}\left[2\sin(800\pi t) - \sin(1600\pi t)\right] \end{aligned} \tag{34}$$

The total energy variation of the DC-3ΦAC MMC is

$$\Delta e_{total2} = \max\left(e_{total2}(t)\right) - \min\left(e_{total2}(t)\right) = 46.6 \text{ kJ} \tag{35}$$

The total energy variation related to the output AC frequency f_1 is

$$\Delta e_{total2} = \frac{18621}{f_1} \text{kJ} \tag{36}$$

For DC-1ΦAC MMC shown in Fig. 8, the total energy is

$$\begin{aligned} e_{total3} &= n_{arm3} \int u_{arm3} i_{arm3} dt \\ &= 4 \times 22.3 \times 0.5 \times \frac{1}{1600\pi}\left[2\sin(800\pi t) - \sin(1600\pi t)\right] \end{aligned} \tag{37}$$

The total energy variation at 400 Hz and the expression related to the output AC frequency f_1 of the DC-1ΦAC MMC is the same as DC-3ΦAC MMC

$$\Delta e_{total3} = \max\left(e_{total3}(t)\right) - \min\left(e_{total3}(t)\right) = 46.6 \text{ kJ} \tag{38}$$

$$\Delta e_{total3} = \frac{18621}{f_1} \text{kJ} \tag{39}$$

For the energy variation calculations of the AC-AC MMC, use the same voltage transfer ratio p which acquires the minimum total switching power as shown in section III.B. Thus for 3ΦAC-3ΦAC MMC as shown in Fig. 9, when voltage transfer ratio p_1 equals 1

$$\begin{aligned} e_{total4} &= n_{arm4} \int u_{arm4} i_{arm4} dt \\ &= \frac{9 \times 26.9 \times 0.37}{1600\pi \times 2}\left[8\sin(200\pi t) - \sin(1600\pi t + 2\varphi)\right] \end{aligned} \tag{40}$$

The total energy variation at 400 Hz is

$$\Delta e_{total4} = \max\left(e_{total4}(t)\right) - \min\left(e_{total4}(t)\right) = 161 \text{kJ} \tag{41}$$

The total energy variation as an expression of output frequency is

$$\Delta e_{total4} = 143.2 + \frac{7162}{f_1} \text{kJ} \tag{42}$$

For 3ΦAC-1ΦAC MMC as shown in Fig. 10, following a similar derivation procedure, the total energy variation at 400 Hz and its expression as a function of output frequency are

$$\Delta e_{total5} = \max\left(e_{total5}(t)\right) - \min\left(e_{total5}(t)\right) = 161 \text{kJ} \tag{43}$$

$$\Delta e_{total5} = 143.2 + \frac{7162}{f_1} \text{kJ} \tag{44}$$

V. Comparison Results

Summarizing the calculation results in section III and section IV:

Authorized licensed use limited to: TU Delft Library. Downloaded on April 03,2024 at 06:49:34 UTC from IEEE Xplore. Restrictions apply.

TABLE I. MMC-SST TOPOLOGIES RATING COMPARISON

SST topologies	MMC rating		
	Total semiconductor ratings (MVA)	*Total capacitor energy ripple (kJ) (Proportional to total capacitance)*	
		400 Hz	*5000 Hz*
BtB MMC (HB-SM)	1080	419	376
DC-3ΦAC MMC (HB-SM)	540	46.6	3.7
DC-1ΦAC MMC (HB-SM)	540	46.6	3.7
3ΦAC-3ΦAC MMC (FB-SM)	1440	161	144
3ΦAC-1ΦAC MMC (FB-SM)	1440	161	144

Note: FB – full bridge, HB – half bridge, SM – submodule

According to Table 1, though capacitor ratings of direct AC-AC MMC based SSTs are lower than the BtB MMC based SST, their total semiconductor ratings are much higher than their counterparts. And because of the complexity of the control system to control two different frequency components, there are no clear benefits for using AC-AC MMC based SST.

As for DRU-MMC based SST, one may find it counterintuitive that the total capacitance requirement for DRU-MMC based SST is not half of the BtB MMC, but much lower than that, which is different from HVDC applications. The reason is that in SST, the medium frequency side MMC has much lower capacitor energy ripple compared to the source side MMC (inversely proportional to the fundamental frequency of the MMC).

Another merit of choosing DRU-MMC based topology is that because of the unidirectional power flow requirement of the electrolyzer application requirement, DRU could be used to replace the source side MMC of the BtB configuration. And because with the same current and voltage rating, the diodes will be much cheaper than IGBT. Thus the DRU-MMC will be much cheaper than the BtB configuration.

Among DC-3ΦAC MMC and DC-1ΦAC MMC, three phase transformers generally have higher power density than single phase transformers. Therefore, DRU – 3Φ MMC based SST is considered the most promising topology and will be prioritized in future SST design.

Note that because of the specific application that this paper focuses on, the compared topologies are mainly unidirectional power flow ones. For the bidirectional power flow SST design, the switches rating calculation will be the same as shown above, but because of the active switches being used, the total price will be undoubtedly increasing, and the capacitor rating will depend on specific structures that are being applied.

VI. CONCLUSION

This paper compares five different MMC based SST topologies for AC-DC applications such as electrolyzers, focusing on power semiconductor ratings and capacitor ratings calculations. According to the comparison results, the emerging AC-AC MMC based SST is found to have lower capacitance requirements but higher semiconductor ratings compared to the traditional BtB configuration. The semiconductor cost of BtB SST could be further reduced by replacing the source side MMC with DRU, owing to the unidirectional power flow requirement, which yields the DRU-MMC based SST topologies. And the DRU-MMC based SST topologies have much lower capacitance requirement than half the BtB MMC capacitance requirement, because of the high fundamental operating frequency required by MFT. In summary, the DRU-MMC based SST topology has the lowest semiconductor cost and capacitance requirement, thus it is deemed as the most suitable topology for unidirectional AC-DC SST applications.

REFERENCES

[1] B. Yodwong, D. Guilbert, M. Phattanasak, W. Kaewmanee, M. Hinaje, and G. Vitale, "AC-DC converters for electrolyzer applications: State of the art and future challenges," *Electronics,* vol. 9, no. 6, p. 912, 2020.

[2] J. Saha, G. N. B. Yadav, and S. K. Panda, "A review on bidirectional matrix-based AC-DC conversion for modular solid-state-transformers," in *2019 IEEE 4th International Future Energy Electronics Conference (IFEEC)*, 2019: IEEE, pp. 1-8.

[3] J. Kucka, D. Karwatzki, and A. Mertens, "AC/AC modular multilevel converters in wind energy applications: Design considerations," in *2016 18th European Conference on Power Electronics and Applications (EPE'16 ECCE Europe)*, 5-9 Sept. 2016 2016, pp. 1-10, doi: 10.1109/EPE.2016.7695542.

[4] L. Baruschka and A. Mertens, "Comparison of Cascaded H-Bridge and Modular Multilevel Converters for BESS application," in *2011 IEEE Energy Conversion Congress and Exposition*, 17-22 Sept. 2011 2011, pp. 909-916, doi: 10.1109/ECCE.2011.6063868.

[5] L. Baruschka and A. Mertens, "A new 3-phase AC/AC modular multilevel converter with six branches in hexagonal configuration," in *2011 IEEE Energy Conversion Congress and Exposition*, 17-22 Sept. 2011 2011, pp. 4005-4012, doi: 10.1109/ECCE.2011.6064314.

[6] K. Ilves, L. Bessegato, and S. Norrga, "Comparison of cascaded multilevel converter topologies for AC/AC conversion," in *2014 International Power Electronics Conference (IPEC-Hiroshima 2014 - ECCE ASIA)*, 18-21 May 2014 2014, pp. 1087-1094, doi: 10.1109/IPEC.2014.6869722.

[7] S. Liu, X. Wang, B. Wang, P. Sun, Q. Zhou, and Y. Cui, "Comparison between back-to-back MMC and M3C as high power AC/AC converters," *2016 IEEE PES Asia-Pacific Power and Energy Engineering Conference (APPEEC),* pp. 671-676, 2016.

[8] H. Akagi, "Classification, terminology, and application of the modular multilevel cascade converter (MMCC)," in *The 2010 International Power Electronics Conference - ECCE ASIA -*, 21-24 June 2010 2010, pp. 508-515, doi: 10.1109/IPEC.2010.5543243.

[9] T. E. Slettbakk, "Development of a Power Quality Conditioning System for Particle Accelerators," Norwegian U. Sci. Tech., 2018.

[10] L. Bessegato, K. Ilves, L. Harnefors, S. Norrga, and S. Östlund, "Control and Admittance Modeling of an AC/AC Modular Multilevel Converter for Railway Supplies," *IEEE Transactions on Power Electronics,* vol. 35, no. 3, pp. 2411-2423, 2020, doi: 10.1109/TPEL.2019.2930321.

[11] Z. He, P. Guo, Z. Shuai, Q. Xu, A. Luo, and J. M. Guerrero, "Modulated Model Predictive Control for Modular Multilevel AC/AC Converter," *IEEE Transactions on Power Electronics,* vol. 34, no. 10, pp. 10359-10372, 2019, doi: 10.1109/TPEL.2019.2895224.

Authorized licensed use limited to: TU Delft Library. Downloaded on April 03,2024 at 06:49:34 UTC from IEEE Xplore. Restrictions apply.